



**HAL**  
open science

## **Lack of NKG2D in MAGT1-deficient patients is caused by hypoglycosylation**

Eline Blommaert, Natalia A Cherepanova, Frederik Staels, Matthew P Wilson, Reid Gilmore, Rik Schrijvers, Jaak Jaeken, François Foulquier, Gert Matthijs

► **To cite this version:**

Eline Blommaert, Natalia A Cherepanova, Frederik Staels, Matthew P Wilson, Reid Gilmore, et al.. Lack of NKG2D in MAGT1-deficient patients is caused by hypoglycosylation. *Human Genetics*, 2022, 141 (7), pp.1279-1286. 10.1007/s00439-021-02400-1 . hal-04473633

**HAL Id: hal-04473633**

**<https://hal.science/hal-04473633v1>**

Submitted on 22 Feb 2024

**HAL** is a multi-disciplinary open access archive for the deposit and dissemination of scientific research documents, whether they are published or not. The documents may come from teaching and research institutions in France or abroad, or from public or private research centers.

L'archive ouverte pluridisciplinaire **HAL**, est destinée au dépôt et à la diffusion de documents scientifiques de niveau recherche, publiés ou non, émanant des établissements d'enseignement et de recherche français ou étrangers, des laboratoires publics ou privés.

1 **Human Genetics – Special issue on Inherited Metabolic Diseases**

2 **Title: MAGT1-deficiency: lack of NKG2D is caused by hypoglycosylation**

3 **Authors**

4 Eline Blommaert<sup>1</sup>, Natalia A. Cherepanova<sup>2</sup>, Frederik Staels<sup>3</sup>, Matthew P. Wilson<sup>1</sup>, Jaak

5 Jaeken<sup>4</sup>, François Foulquier<sup>5</sup>, Rik Schrijvers<sup>3</sup>, Reid Gilmore<sup>2</sup> and Gert Matthijs<sup>1</sup>

6 <sup>1</sup>Laboratory for Molecular Diagnosis, Center for Human Genetics, KU Leuven, 3000 Leuven, Belgium

7 <sup>2</sup>Department of Biochemistry and Molecular Pharmacology, University of Massachusetts Medical School,

8 01655 Worcester, MA, USA

9 <sup>3</sup> KU Leuven department of microbiology, immunology and transplantation, Allergy and Clinical Immunology

10 research group, KU Leuven, 3000 Leuven, Belgium

11 <sup>4</sup> Department of Pediatrics, Center for Metabolic Diseases, KU Leuven, 3000 Leuven, Belgium

12 <sup>5</sup> Univ. Lille, CNRS, UMR 8576 – UGSF - Unité de Glycobiologie Structurale et Fonctionnelle, F- 59000 Lille,

13 France

14 **Corresponding Author**

15 Gert Matthijs, Herestraat 49 O&N 1 Box 606, 3000 Leuven, Belgium, +32 16 34 60 70,

16 [gert.matthijs@kuleuven.be](mailto:gert.matthijs@kuleuven.be)

17 **Supplementary data:** yes

18 1 Supplementary Information file (pdf format)

19

20 **Abstract**

21 Mutations in the X-linked gene *MAGT1* cause a Congenital Disorder of Glycosylation (CDG),  
22 with two distinct clinical phenotypes: a primary immunodeficiency (XMEN disorder) versus  
23 intellectual and developmental disability. It was previously established that *MAGT1*  
24 deficiency abolishes steady state expression of the immune response protein NKG2D  
25 (encoded by *KLRK1*) in lymphocytes. Here, we show that the reduced steady state levels of  
26 NKG2D are caused by hypoglycosylation of the protein and we pinpoint the exact site that is  
27 underglycosylated in *MAGT1*-deficient patients. Furthermore, we challenge the possibility  
28 that supplementation with magnesium restores NKG2D levels and show that addition of this  
29 ion does not significantly improve NKG2D steady state expression nor does it rescue the  
30 hypoglycosylation defect in knock out human cell lines. Moreover, magnesium  
31 supplementation of an XMEN patient did not result in restoration of NKG2D expression on  
32 the cell surface of lymphocytes. In summary, we demonstrate that in *MAGT1*-deficient  
33 patients the lack of NKG2D is caused by hypoglycosylation.

34

35 **Keywords**

36 CDG, OST, STT3B, *MAGT1*, XMEN, NKG2D

37

38 **Declarations**

39 **Funding**

40 This research was supported by Research Foundation Flanders (FWO): under the frame of E-  
41 Rare-3, the ERA-Net for Research on Rare Diseases (ERA-NET Cofund action N°64578) (to  
42 GM), a research stay grant (FWO V417818N) (to EB), a senior clinical investigator fellowship  
43 (to RS), and GLYCO4DIAG, an International Associated Laboratory grant from National Centre  
44 for Scientific Research (CNRS) and FWO (to FF and GM). The work was also supported by the  
45 National Institute of General Medical Sciences of the National Institutes of Health under  
46 award number GM43768 (to RG), C1 KU Leuven fund (to RS) and by the JAEKEN-THEUNISSEN  
47 CDG FUND.

48 **Conflict of interest**

49 The authors declare no conflict of interest.

50 **Availability of data and material**

51 Not applicable

52

53 **Code availability**

54 Not applicable

55 **Author contributions**

56 Designed the experiments: EB, NAC, FS, RG and RS. Performed the experiments: EB, NAC, FS  
57 and MW. Analysed the data: EB and NAC. EB wrote the manuscript with support from JJ, FF  
58 and GM. Clinical evaluation of patient: RS. All authors discussed and revised the manuscript.

59 **Ethics approval**

60 Research on patient cells was approved by the Ethical Committee of the University Hospital  
61 of Leuven (approval number S58466).

62 **Consent for publication**

63 The patient and controls in this study provided informed consent.

## 64 **Introduction**

65 MAGT1 is a controversial protein with two described and intrinsically conflicting roles: it has  
66 been shown that MAGT1 is a subunit of the STT3B oligosaccharyltransferase (OST) complex  
67 at the endoplasmic reticulum (Kelleher et al. 2003; Cherepanova et al. 2014). However,  
68 MAGT1 was also described as a plasma membrane localised magnesium ( $Mg^{2+}$ ) transporter  
69 (Goytain and Quamme 2005; Zhou and Clapham 2009). Patients with mutations in *MAGT1*  
70 present with two distinct phenotypes; a primary immunodeficiency characterised by  
71 chronic-active EBV infections (XMEN disorder) (Li et al. 2011) and a strikingly different  
72 phenotype where patients present with intellectual and developmental disability  
73 (Blommaert et al. 2019). Recently, we demonstrated that in both clinical presentations, N-  
74 glycosylation is affected. The disorder, MAGT1-CDG, therefore falls under the umbrella of  
75 the Congenital Disorders of Glycosylation (CDG) (Blommaert et al. 2019).

76 CDG are a group of genetic disorders with defects in the synthesis or attachment of glycans  
77 onto glycoproteins and glycolipids. They show a great variety of clinical presentations with  
78 involvement of multiple organs and tissues (Freeze et al. 2014; Jaeken and Péanne 2017). In  
79 the N-glycosylation pathway, the enzymes constituting the OST are responsible for the  
80 transfer of glycans from a dolichol carrier onto proteins at specific Asn residues recognised  
81 by the Asn-X-Ser/Thr motif (Aebi 2013). The OST is a multimeric complex with two different  
82 catalytic subunits, STT3A and STT3B. Each of these assemble into their own complex. Some  
83 accessory subunits are present in both and others are specific for each respective catalytic  
84 unit (Kelleher et al. 2003). MAGT1 is an isoform-specific subunit of STT3B with an  
85 oxidoreductase domain and is crucial for the functioning of the STT3B OST complex  
86 (Cherepanova et al. 2014; Cherepanova and Gilmore 2016). Interestingly, TUSC3 is a  
87 homologue of MAGT1 that is able to perform the same role, but has a more restricted

88 expression profile (Zhou and Clapham 2009; Matsuda-Lennikov et al. 2019). Thus, mutations  
89 in *MAGT1* lead to a glycosylation defect caused by dysfunctional STT3B-dependent  
90 glycosylation, but only in absence of TUSC3 expression (Blommaert et al. 2019).

91 Understanding the pathophysiological consequences of a disordered glycosylation  
92 machinery is particularly challenging, as it is estimated that 50% of the proteome is  
93 glycosylated and many downstream pathways are affected (Petrescu et al. 2006; Jaeken and  
94 Péanne 2017). The investigation of two *MAGT1*-deficient XMEN patients demonstrated that  
95 steady state expression of the immune response NKG2D protein is impaired; it was therefore  
96 postulated that reduced expression of NKG2D leads to increased susceptibility to EBV  
97 infections (Chaigne-Delalande et al. 2013). NKG2D is encoded by *KLRK1*, and expression of  
98 this protein is restricted to CD8<sup>+</sup> T cells, NK, NKT and subsets of  $\gamma\delta$  T cells. NKG2D forms a  
99 homodimer of two disulphide-linked transmembrane proteins (Garrity et al. 2005). The  
100 protein itself does not have signalling properties, instead it associates with a signalling  
101 subunit, DAP10; this in turn activates several intracellular cascades such as the  
102 phosphatidylinositol-3-kinase pathway (Wu et al. 1999). Cellular stress, *e.g.* due to  
103 bacterial/viral infections, or malignantly transformed cells, cause an upregulation of NKG2D  
104 ligands (Jamieson et al. 2002; Raulet et al. 2013). As reduced levels of intracellular free Mg<sup>2+</sup>  
105 concentrations were measured in XMEN patients (Li et al. 2011), supplementation with Mg<sup>2+</sup>  
106 was proposed as a potential therapy. Upon addition of an excess concentration of Mg<sup>2+</sup>,  
107 NKG2D steady state levels were restored in defective CD8<sup>+</sup> and NK cells. Interestingly,  
108 patients receiving Mg<sup>2+</sup> supplementation *in vivo* also presented with increased levels of  
109 NKG2D expression (Chaigne-Delalande et al. 2013).

110 In light of the newly gained knowledge that *MAGT1* mutations cause a glycosylation defect  
111 in XMEN disorder (Blommaert et al. 2019; Matsuda-Lennikov et al. 2019), we studied the

112 glycosylation status and protein expression of NKG2D, using HEK293 cells knocked out for  
113 different subunits of the OST. We hypothesised that the lack of NKG2D expression in patient  
114 CD8<sup>+</sup> and NK cells is due to hypoglycosylation of the protein, caused by mutations in MAGT1.  
115 Furthermore, we assayed the effects of Mg<sup>2+</sup> supplementation on NKG2D expression in an  
116 XMEN patient.

## 117 **Material and methods**

### 118 **Patient and cells**

119 CRISPR-Cas9 engineered HEK293 WT cells, depleted for either STT3A, STT3B, MAGT1 and TUSC3 were  
120 previously described (Cherepanova and Gilmore 2016). HEK293 cells were cultured in Dulbecco's  
121 modified Eagle medium (Life Technologies), supplemented with 10% fetal bovine serum (Clone III,  
122 HyClones) at 37°C under 5% CO<sub>2</sub>. Peripheral Blood Mononuclear Cells (PBMCs) from patient 1 and  
123 healthy controls were isolated using Lymphocyte Separation Medium (MP Biomedicals). Patient cells  
124 were isolated during routine outpatient visits, in the absence of intercurrent illnesses, without (at  
125 time point 0) and with Mg-gluconate 3 g QD oral substitution (containing 162 mg Mg<sup>2+</sup>) at different  
126 time points. Clinical synopsis is described in greater detail in the supplementary data.

### 127 **Epstein-Barr Virus quantification**

128 DNA was extracted from whole blood (EDTA) using QIAAsymphonySP/AS (Qiagen) followed by  
129 quantification using RT-PCR Taqman on QuantStudio Dx (Thermo Fisher Scientific).

### 130 **Expression vectors**

131 NKG2D-Myc-DDK and DAP10-Myc-DDK expression plasmids were purchased from Origene.  
132 Elimination of glycosylation sites was achieved by introducing asparagine to glutamine  
133 mutations using site-directed mutagenesis to obtain the NKG2D-Myc-DDK N131AS (N108Q,



134 N163Q, N202Q), N163QS (N108Q, N131Q, N202Q), N202CS (N108Q, N131Q, N163Q) and  
135  $\Delta$ N108CS (N108Q) mutants. The mutations were confirmed by Sanger sequencing.

### 136 **Protein expression**

137 HEK293 cells were seeded in 6-well or 60 mm dishes 24h prior to transfection. Plasmid  
138 transfection was performed using 6  $\mu$ g plasmid (60 mm dish) and Lipofectamine 3000  
139 (Invitrogen) in serum-free Opti-MEM medium (GIBCO) according to the manufacturer's  
140 instructions. Cotransfections were performed with 1.5  $\mu$ g of each vector (6-well). Cells were  
141 assayed 24h later for pulse chase labelling, 48h later for immunoblotting.

### 142 **Antibodies**

143 Anti-NKG2D N20 (sc-9621) polyclonal antibody was purchased from Santa Cruz  
144 Biotechnology, goat polyclonal antisera specific for CatC (AF1071) from R&D Systems and  
145 mouse monoclonal antisera for  $\beta$ -tubulin (ab101019) from Abcam. Anti-STT3B and anti-  
146 STT3A antibodies were described previously (Kelleher et al. 2003). For recognition of epitope  
147 tags anti-DDK (F3165 anti-FLAG M2, Sigma) was used.

### 148 **Immunoblotting**

149 Cells were lysed in RIPA buffer (50 mM Tris-HCl pH=7.5, 150 mM NaCl, 1% NP-40, 0.5%  
150 sodium deoxycholate, 0.1% SDS), supplemented with protease and phosphatase inhibitors  
151 (Thermo Fisher Scientific). Protein content was quantified using the Micro BCA Protein Assay  
152 Kit (Thermo Fisher Scientific). 20  $\mu$ g of proteins were immunoblotted onto a nitrocellulose  
153 membrane (Thermo Fisher Scientific). Signals were detected using Western Lightning-ECL  
154 (Perkin Elmer) and autoradiographed with ImageQuant LAS4000, band intensities were  
155 measured using ImageQuant TL (both GE Healthcare). To calculate the total NKG2D levels,

156 the whole area –from the fully glycosylated to the completely hypoglycosylated protein –  
157 was taken into account.

### 158 **Pulse-chase radiolabelling**

159 Expression vectors were pulse-chase labelled with Tran<sup>35</sup>S label (Perkin Elmer), as previously  
160 described (Cherepanova et al. 2014). Dry gels were exposed to a phosphor screen (Fujifilm),  
161 scanned in Typhoon FLA 9000, and quantified using ImageQuant TL (GE Healthcare).  
162 Endoglycosidase H was used as a mobility marker, according to manufacturers' instructions  
163 (New England BioLabs).

### 164 **Flow cytometry**

165 After thawing of PBMCs, cells were washed in dPBS supplemented with 0.5% BSA. The cells  
166 were stained with anti-CD19 (clone 1D3, 557398, BD biosciences) and anti-CD56 (Clone  
167 CMSSB, 46-0567-42), anti-CD16 (clone eBioB16, 17-0168-42), anti-CD4 (clone OKT4, 56-  
168 0048-41), anti-CD8 (clone SK1, 48-0087-42; clone RPA-T8, 56-0088-41) and anti-CD3 (clone  
169 OKT3, 86-0037-42) (all eBioscience); anti-NKG2D (clone 1D11, 320806), anti-CD2 (clone  
170 TS1/8, 309214), anti-CD3 PE Cy7 (300420) (all Biolegend); anti-CD56 PerCP e71 (46-0566-41)  
171 (Thermo Fisher Scientific). FVD 780 APC-Cy7 (Thermo Fisher Scientific) was used for  
172 live/dead staining. Data were collected on a BD LSR Fortessa and analysed using FlowJo  
173 V.10.5 (Tree Star Inc.).

### 174 **Statistics**

175 Statistical analyses were performed in R (version 3.6.2). Individual data points between two  
176 groups were analysed by Welch Student's t test, samples before and after treatment by  
177 paired Student's t test.  $p < 0.05$  was considered significant.

178

## 179 Results

### 180 1 NKG2D is an STT3B-dependent glycoprotein

181 It has previously been shown that steady state levels of NKG2D in CD8<sup>+</sup> lymphocytes and NK  
182 cells from XMEN patients were severely decreased (Chaigne-Delalande et al. 2013). By  
183 immunoblotting, it was observed that NKG2D is absent in both CD8<sup>+</sup> and NK cell lysates of  
184 MAGT1-deficient patients, but that a ~8 kDa lighter isoform was present. From this we  
185 hypothesise that this isoform is the hypoglycosylated protein. NKG2D is a 216 residue  
186 protein that has four N-glycosylation sites (N<sub>108</sub>NC, N<sub>131</sub>AS, N<sub>163</sub>GS, N<sub>202</sub>CS), of which one is a  
187 suboptimal sequon (N<sub>108</sub>NC) (**Fig. 1a**).

188 Different KO HEK293 cell lines (STT3A<sup>-/-</sup>, STT3B<sup>-/-</sup> and the double KO MAGT1<sup>-/-</sup>TUSC3<sup>-/-</sup>)  
189 (Cherepanova and Gilmore 2016), were used as cellular model to assess the glycosylation  
190 status of NKG2D. The MAGT1<sup>-/-</sup>TUSC3<sup>-/-</sup> HEK293 cell line was preferred over MAGT1<sup>-/-</sup> cells,  
191 as TUSC3 expression rescues the glycosylation defect caused by MAGT1-deficiency  
192 (Cherepanova and Gilmore 2016; Blommaert et al. 2019). Each HEK293 cell line was  
193 transfected with a NKG2D-Myc-DDK construct, followed by metabolic pulse-chase labelling.  
194 Treatment with endoglycosidase H (EH) was used to remove all glycans and represents a  
195 mobility marker for the fully hypoglycosylated form of NKG2D. **Fig. 1b** shows that for NKG2D  
196 transfected in WT cells, the most abundant form carries 3 glycans. A faint, slower migrating  
197 band can be observed, where the protein carries 4 glycans. This 4<sup>th</sup> glycosylation site is the  
198 suboptimal N<sub>108</sub>NC sequon, as radiolabelling of NKG2D-ΔN<sub>108</sub>NC-Myc-DDK showed that the  
199 protein carries 3 glycans (**Fig. S2**). In the MAGT1<sup>-/-</sup>TUSC3<sup>-/-</sup> and STT3B<sup>-/-</sup> cells, multiple  
200 hypoglycosylated forms appear (average number of glycans is in both cell lines 1.3,  
201 compared to 3.1 in WT). In contrast, NKG2D is fully glycosylated in STT3A<sup>-/-</sup> cells (average  
202 number of glycans is 2.9).

203 To pinpoint the N-glycosylation sequons that are strictly STT3B-dependent, we proceeded by  
204 generating three NKG2D mutant constructs, where all sequons were removed by  
205 mutagenesis except one (N<sub>131</sub>AS, N<sub>163</sub>GS or N<sub>202</sub>CS). The different HEK293 cell lines were  
206 transfected with these constructs, followed by pulse-chase labelling. **Fig. 1c** shows that the  
207 N<sub>202</sub>CS NKG2D construct is completely hypoglycosylated in the MAGT1<sup>-/-</sup>TUSC3<sup>-/-</sup> and STT3B<sup>-/-</sup>  
208 HEK293 cells. In the other constructs, N<sub>131</sub>AS and N<sub>163</sub>GS, a doublet appears in the STT3B<sup>-/-</sup>  
209 and MAGT1<sup>-/-</sup>TUSC3<sup>-/-</sup> cells, indicating a partial block in STT3B dependent glycosylation  
210 (ranging from 20 to 40% reduction of glycosylation compared to WT cells). In summary,  
211 these results indicate that NKG2D is a glycoprotein with one sequon (N<sub>202</sub>CS) that is strictly  
212 STT3B and MAGT1/TUSC3-dependent, and two others that are partially.

## 213 **2 NKG2D steady state expression is decreased in cells with a defective STT3B complex**

214 To determine whether the observed hypoglycosylation in MAGT1<sup>-/-</sup>TUSC3<sup>-/-</sup> and STT3B<sup>-/-</sup> cells  
215 has an effect on the protein steady state levels of NKG2D, 48h cotransfection with NKG2D-  
216 myc-DDK and DAP10-myc-DDK, an accessory protein of NKG2D, was performed in the  
217 different KO cell lines, followed by immunoblotting. This revealed that the expression of fully  
218 glycosylated NKG2D is strongly reduced in the MAGT1<sup>-/-</sup>TUSC3<sup>-/-</sup> and STT3B<sup>-/-</sup> cell lines (**Fig.**  
219 **2a, 2c**). In addition, multiple hypoglycosylated bands appear in these KO cell lines (**Fig. 2a**).  
220 Taking the total NKG2D (all the glycoforms) into account, a reduction of more than 70% was  
221 observed in STT3B<sup>-/-</sup> and MAGT1<sup>-/-</sup>TUSC3<sup>-/-</sup> cells, compared to WT. When looking at the  
222 biologically most relevant isoform, the fully glycosylated NKG2D (carrying 3 to 4 glycans),  
223 only 11% and 14% of this isoform was present respectively in MAGT1<sup>-/-</sup>TUSC3<sup>-/-</sup> and STT3B<sup>-/-</sup>  
224 mutants compared to the WT control (**Fig. 2c**). This is in contrast with the relative abundance  
225 of 53% in STT3A<sup>-/-</sup> cells. Altogether, we show that the block in STT3B-dependent  
226 glycosylation causes a strong reduction in NKG2D steady state levels.

### 227 **3 Magnesium supplementation does not rescue NKG2D expression**

228 Supplementation of CD8<sup>+</sup> and NK cells from XMEN patients with 5 mM MgSO<sub>4</sub> restored the  
229 defective expression of NKG2D protein levels (Chaigne-Delalande et al. 2013). To test  
230 whether Mg<sup>2+</sup> supplementation could rescue the observed hypoglycosylation for NKG2D in  
231 STT3B<sup>-/-</sup> and MAGT1<sup>-/-</sup>TUSC3<sup>-/-</sup> cell lines (**Fig. 2a, 2c**), HEK293 cells were cotransfected with  
232 NKG2D-Myc-DDK and DAP10-Myc-DDK, treated with 5 mM MgSO<sub>4</sub> for 48h and analysed by  
233 immunoblotting. A statistically significant increase in the abundance of the fully glycosylated  
234 NKG2D was observed between untreated and Mg<sup>2+</sup> supplemented cells in STT3A<sup>-/-</sup> and  
235 STT3B<sup>-/-</sup> cell lines, however for total NKG2D no statistically significant differences were seen  
236 for the mutant cell lines (**Fig. 2b, 2c**).

237 Previously, we identified an XMEN patient with a pathogenic variant (c.938T>G; p.Leu313\*)  
238 in *MAGT1* (clinical synopsis in **supplementary information** and pedigree shown in **Fig. S1**).  
239 We were able to show that STT3B-dependent substrates were underglycosylated in patient-  
240 derived cell lines. Furthermore, we demonstrated that NKG2D cell surface expression in NK  
241 cells was strongly reduced in P1 compared to healthy controls (Blommaert et al. 2019). The  
242 latter experiment was repeated after treatment of P1 with 3 g Mg-gluconate (containing 162  
243 mg Mg<sup>2+</sup>) per day at 3 and 21 months, and was also performed on CD8<sup>+</sup> lymphocytes. The  
244 supplementation of P1 with Mg<sup>2+</sup> did not significantly increase the levels of NKG2D cell  
245 surface expression compared to the results before supplementation (**Fig. 3a**). Moreover, EBV  
246 viremia levels increased over time and were deemed to be non-responsive to Mg<sup>2+</sup>  
247 supplementation (**Fig. 3b**). Both findings are in contrast with (Chaigne-Delalande et al. 2013),  
248 where *in vivo* treatment resulted in increased NKG2D levels on CD8<sup>+</sup> lymphocytes and lower  
249 EBV<sup>+</sup> B cells. Additional biochemical workup of P1 showed no differences before or after

250 treatment (**Table S1**). However, the patient himself feels better with the magnesium  
251 supplementation.

## 252 **Discussion**

253 MAGT1-deficiency is a remarkable disorder; it is an immunological disease as well as a  
254 glycosylation defect. Therefore, it belongs to the CDG group with major immunological  
255 involvement, such as ALG12-CDG, ATP6AP1-CDG, EXTL3-CDG, FUT8-CDG, G6PC3-CDG,  
256 JAGN1-CDG, MOGS-CDG, PGM3-CDG, SLC35C1-CDG and SLC37A4-CDG (Pascoal et al. 2020).  
257 Since the principal description in 2011 by Li et al., 36 male patients with this X-linked  
258 disease, with 21 different pathogenic variants, have been reported (see review in Ravell et  
259 al. 2020a). The patients have a combined immunodeficiency, clinically characterized by  
260 increased susceptibility to chronic EBV sinopulmonary and ear infections (75%),  
261 lymphadenopathy (53%), EBV-associated lymphoproliferative disease/lymphoma (36%),  
262 splenomegaly (31%), molluscum contagiosum (25%), severe autoimmune cytopenias (25%),  
263 and mouth sores (22%). Other, albeit less frequent, symptoms (19 to 6%) are skin warts,  
264 neurological symptoms (including Guillain-Barré syndrome), bleedings, varicella zoster virus  
265 and herpes simplex virus infections, intellectual/developmental disability, effusions and EBV  
266 negative malignancy. All described patients by Ravell et al. 2020a have decreased NKG2D  
267 expression on natural killer and CD8<sup>+</sup> T cells, and increased (sustained or fluctuating) serum  
268 transaminases.

269 NKG2D is an essential activating receptor in the cytolytic response of immune cells,  
270 expressed in NK and CD8<sup>+</sup> cells, among other cell types. It has been previously demonstrated  
271 that mutations in MAGT1 cause a dramatic decline in NKG2D protein levels (Chaigne-

272 Delalande et al. 2013). NKG2D activity is important for the recognition of EBV infection, and  
273 subsequent activation (Münz 2017). Therefore, it was concluded that XMEN patients are  
274 susceptible to chronic-active EBV viremia, and in some cases the development of EBV-  
275 related lymphoma's, due to the lack of NKG2D expression (Chaigne-Delalande et al. 2013).  
276 By addition of an excess amount of  $MgSO_4$  to NK and  $CD8^+$  cells, NKG2D expression was  
277 restored to similar levels as control samples. As a consequence,  $Mg^{2+}$  supplementation was  
278 explored as a possible treatment for MAGT1-deficient patients. This led to an increase in cell  
279 surface expression of NKG2D in two tested patients, and a decrease in EBV-infected cells  
280 (Chaigne-Delalande et al. 2013).

281 Recently, we demonstrated that in a XMEN patient, as well as in MAGT1-deficient patients  
282 with intellectual and developmental disability, STT3B-dependent glycosylation is affected  
283 due to MAGT1 mutations (Blommaert et al. 2019). Later on, our findings were confirmed by  
284 Matsuda-Lennikov et al. 2019 and Ravell et al. 2020b, showing N-glycosylation defects in  
285 other XMEN patients. Interestingly, the thorough clinical examination of a large XMEN  
286 cohort concluded that this is a complex, multisystem glycosylation disorder, going beyond  
287 the initially described immunodeficiency. The researchers abandoned the  $Mg^{2+}$ -transporter  
288 hypothesis, and agreed with the proposed role of MAGT1 in glycosylation (Matsuda-  
289 Lennikov et al. 2019). This strengthens the research line that MAGT1 is an OST subunit, and  
290 that possibly a downstream  $Mg^{2+}$  homeostasis glycoprotein is hypoglycosylated  
291 (Cherepanova et al. 2016). Here, we focussed on the link between NKG2D and XMEN, to  
292 assess whether its instability is caused by hypoglycosylation.

293 We demonstrated that NKG2D has one sequon ( $N_{202}CS$ ) that is completely dependent on the  
294 STT3B complex (and therefore also on MAGT1) for proper glycosylation, which is in  
295 concordance with previous reports showing that glycosylation sites in the last 65 residues of

296 the C-terminus are strictly STT3B-glycosylated (Cherepanova et al. 2019). Moreover, the  
297 other sites (N<sub>131</sub>AS and N<sub>163</sub>GS) showed a mild dependency on the STT3B complex. We  
298 believe that hypoglycosylation causes the described deficient expression of NKG2D in XMEN  
299 patients. Upon supplementation of 5 mM Mg<sup>2+</sup> no significant restoration of NKG2D could be  
300 observed in MAGT1<sup>-/-</sup>TUSC3<sup>-/-</sup> cells transfected with NKG2D and DAP10. This is in sharp  
301 contrast with the rescue of NKG2D stability in patient lymphocyte cell cultures in a previous  
302 publication (Chaigne-Delalande et al. 2013). We cannot exclude that the high concentration  
303 of Mg<sup>2+</sup> used for this rescue was able to enhance NKG2D expression by indirect effects,  
304 which makes it difficult to reproduce such results as environmental factors likely have an  
305 influence. Unfortunately, stimulation of P1 PBMCs with anti-CD3/CD28 did not result in  
306 proliferation of lymphocytes, therefore we were not able to perform this experiment on  
307 patient cells. Moreover, we showed that *in vivo* treatment of P1 with Mg<sup>2+</sup> did not cause any  
308 significant improvements in NKG2D expression, supporting the data obtained in cell lines.  
309 This is in contrast with the study showing that treatment with Mg-threonate leads to an  
310 increase in NKG2D expression on the cell surface of CD8<sup>+</sup> and NK cells (Chaigne-Delalande et  
311 al. 2013), although in our case Mg-gluconate was used.

312 As NKG2D is important in EBV recognition, the lack of expression of this protein is probably  
313 an important modulator for the typical EBV infections in XMEN patients. In addition, a  
314 glycoproteomic assay in XMEN lymphocytes showed that multiple important immune  
315 regulators, such as CD28 and CD70, were hypoglycosylated, further contributing to the  
316 phenotype. In line with our results shown here, NKG2D was also hypoglycosylated in this  
317 dataset (Ravell et al. 2020b).

318 Remarkably, the previously described MAGT1-CDG patients do not have an immune  
319 phenotype to this date (Blommaert et al. 2019). It would be interesting to study immune



320 glycoproteins from these patients, to determine whether the difference in clinical phenotype  
321 is caused by differences in steady state levels of these proteins. Unfortunately, no  
322 lymphocyte material was available from these patients, leaving room for speculation.

323 In conclusion, we demonstrated that NKG2D glycosylation is dependent on STT3B, and by  
324 extension, of MAGT1. Moreover, we pinpoint the exact sequon that is underglycosylated.

325 The strongly reduced NKG2D expression in patients is, at least partially, responsible for the  
326 susceptibility of MAGT1-deficient patients to EBV infections. Thus, we were able to link the  
327 pathological mechanism (hypoglycosylation) in XMEN patients to the clinical phenotype.

328 **References**

- 329 Aebi M (2013) N-linked protein glycosylation in the ER. *Biochim Biophys Acta - Mol Cell Res*  
330 1833:2430–2437. <https://doi.org/10.1016/j.bbamcr.2013.04.001>
- 331 Blommaert E, Péanne R, Cherepanova NA, et al (2019) Mutations in MAGT1 lead to a  
332 glycosylation disorder with a variable phenotype. *Proc Natl Acad Sci* 116:9865–9870.  
333 <https://doi.org/10.1073/pnas.1817815116>
- 334 Chaigne-Delalande B, Li F-Y., O' Connor GM., et al (2013) Mg<sup>2+</sup> regulates cytotoxic functions  
335 of NK and CD8 T cells in chronic EBV infection through NKG2D. *Science* (80- ) 341:186–  
336 191
- 337 Cherepanova NA, Gilmore R (2016) Mammalian cells lacking either the cotranslational or  
338 posttranslocational oligosaccharyltransferase complex display substrate-dependent  
339 defects in asparagine linked glycosylation. *Sci Rep* 6:20946:1–12.  
340 <https://doi.org/10.1038/srep20946>
- 341 Cherepanova NA, Shrimal S, Gilmore R (2014) Oxidoreductase activity is necessary for N-  
342 glycosylation of cysteine-proximal acceptor sites in glycoproteins. *J Cell Biol* 206:525–  
343 39. <https://doi.org/10.1083/jcb.201404083>
- 344 Cherepanova NA, Shrimal S, Gilmore R (2016) N-linked glycosylation and homeostasis of the  
345 endoplasmic reticulum. *Curr Opin Cell Biol* 41:57–65.  
346 <https://doi.org/10.1016/j.ceb.2016.03.021>
- 347 Cherepanova NA, Venev S V, Leszyk JD, et al (2019) Quantitative glycoproteomics reveals  
348 new classes of STT3A- and STT3B-dependent N-glycosylation sites. *J Cell Biol* 1–15
- 349 Freeze HH, Chong JX, Bamshad MJ, Ng BG (2014) Solving glycosylation disorders:  
350 fundamental approaches reveal complicated pathways. *Am J Hum Genet* 94:161–75.  
351 <https://doi.org/10.1016/j.ajhg.2013.10.024>

352 Garrity D, Call ME, Feng J, Wucherpfennig KW (2005) The activating NKG2D receptor  
353 assembles in the membrane with two signaling dimers into a hexameric structure. *Proc*  
354 *Natl Acad Sci U S A* 102:7641–7646. <https://doi.org/10.1073/pnas.0502439102>

355 Goytain A, Quamme GA (2005) Identification and characterization of a novel mammalian  
356 Mg<sup>2+</sup> transporter with channel-like properties. *BMC Genomics* 1:48.  
357 <https://doi.org/10.1186/1471-2164-6-48>

358 Jaeken J, Péanne R (2017) What is new in CDG? *J Inherit Metab Dis* 40:569–586.  
359 <https://doi.org/10.1007/s10545-017-0050-6>

360 Jamieson AM, Diefenbach A, McMahon CW, et al (2002) The Role of the NKG2D  
361 Immunoreceptor in Immune Cell Activation and Natural Killing. *Immunity* 17:19–29

362 Kelleher DJ, Karaoglu D, Mandon EC, Gilmore R (2003) Oligosaccharyltransferase isoforms  
363 that contain different catalytic STT3 subunits have distinct enzymatic properties. *Mol*  
364 *Cell* 12:101–111. [https://doi.org/10.1016/S1097-2765\(03\)00243-0](https://doi.org/10.1016/S1097-2765(03)00243-0)

365 Li F-Y, Chaigne-Delalande B, Kanellopoulou C, et al (2011) Second messenger role for Mg<sup>2+</sup>  
366 revealed by human T-cell immunodeficiency. *Nature* 475:471–476.  
367 <https://doi.org/10.1038/nature10246>

368 Matsuda-Lennikov M, Biancalana M, Zou J, et al (2019) Magnesium transporter 1 (MAGT1)  
369 deficiency causes selective defects in N-linked glycosylation and expression of immune-  
370 response genes. *J Biol Chem* 1:jbc.RA119.008903.  
371 <https://doi.org/10.1074/jbc.RA119.008903>

372 Münz C (2017) Epstein-Barr virus-specific immune control by innate lymphocytes. *Front*  
373 *Immunol* 8:1658: 1–7. <https://doi.org/10.3389/fimmu.2017.01658>

374 Pascoal C, Francisco R, Ferro T, et al (2020) CDG and immune response: From bedside to  
375 bench and back. *J Inherit Metab Dis* 43:90–124. <https://doi.org/10.1002/jimd.12126>

376 Petrescu A-J, Wormald MR, Dwek R a (2006) Structural aspects of glycomes with a focus on  
377 N-glycosylation and glycoprotein folding. *Curr Opin Struct Biol* 16:600–7.  
378 <https://doi.org/10.1016/j.sbi.2006.08.007>

379 Raulet DH, Gasser S, Gowen BG, et al (2013) Regulation of ligands for the activating receptor  
380 NKG2D

381 Ravell JC, Chauvin SD, He T, Lenardo M (2020a) An Update on XMEN Disease. *J Clin Immunol*  
382 40:671–681. <https://doi.org/10.1007/s10875-020-00790-x>

383 Ravell JC, Matsuda-Lennikov M, Chauvin SD, et al (2020b) Defective glycosylation and  
384 multisystem abnormalities characterize the primary immunodeficiency XMEN disease. *J*  
385 *Clin Invest* 130:507–522. <https://doi.org/10.1172/JCI131116>

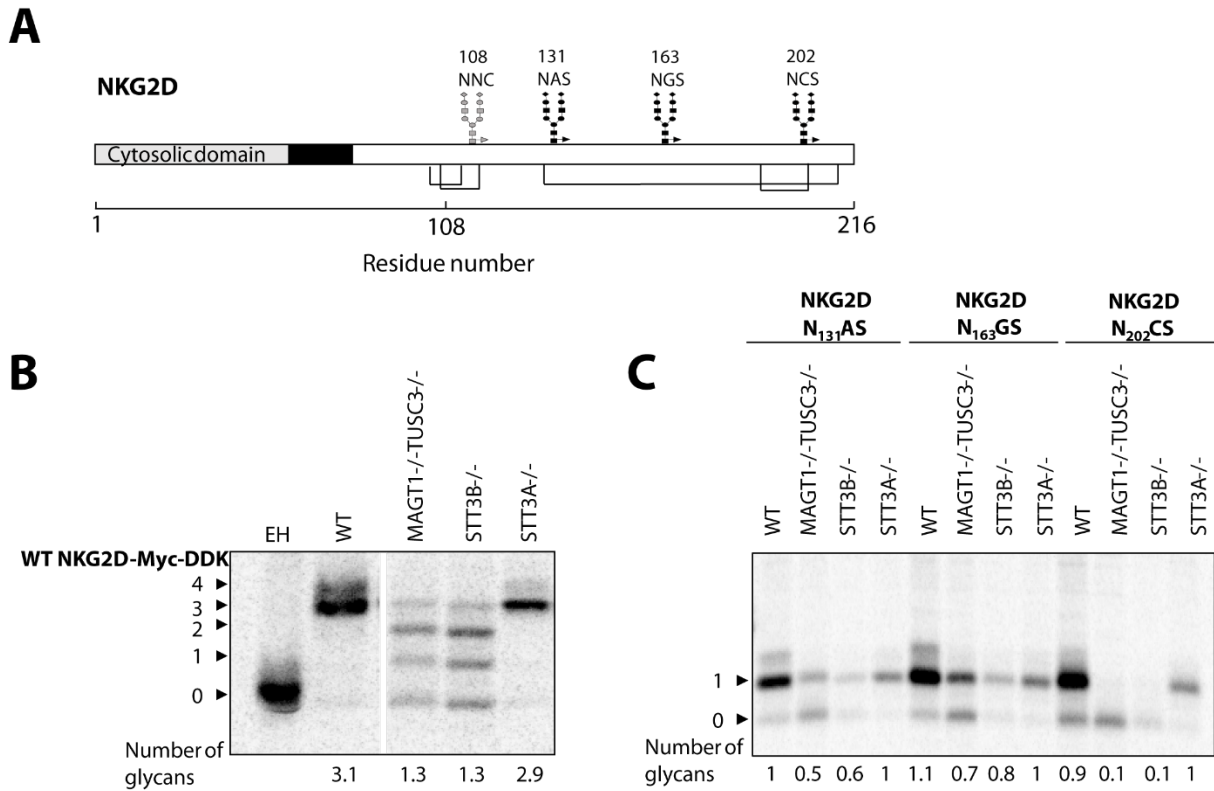
386 Ruiz-Canada C, Kelleher DJ, Gilmore R (2009) Cotranslational and Posttranslational N-  
387 Glycosylation of Polypeptides by Distinct Mammalian OST Isoforms. *Cell* 136:272–283.  
388 <https://doi.org/10.1016/j.cell.2008.11.047>

389 Wu J, Song Y, Bakker ABH, et al (1999) An Activating Immunoreceptor Complex Formed by  
390 NKG2D and DAP10. *Science* (80- ) 285:730–732.  
391 <https://doi.org/10.1126/science.285.5428.730>

392 Zhou H, Clapham DE (2009) Mammalian MagT1 and TUSC3 are required for cellular  
393 magnesium uptake and vertebrate embryonic development. *Proc Natl Acad Sci U S A*  
394 106:15750–5. <https://doi.org/10.1073/pnas.0908332106>

395

396

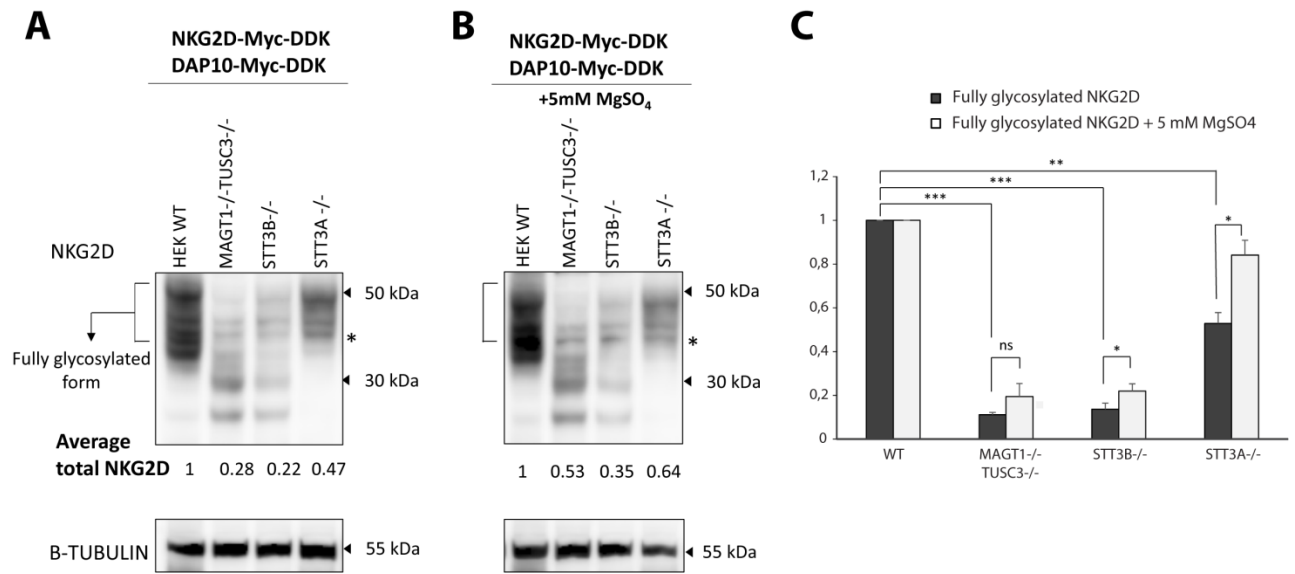


398

399 **Fig. 1 NKG2D is hypoglycosylated in cells lacking STT3B activity**

400 **(a)** Diagram showing the glycosylation sites of NKG2D. Grey glycan indicates a suboptimal glycosylation sequon  
 401 ( $N_{108}NC$ ). The transmembrane domain is depicted in black, cysteine residues by black lines. **(b)** WT and KO  
 402 HEK293 cells were transfected with NKG2D-Myc-DDK followed by metabolic pulse-chase labelling. The figure  
 403 was spliced between the WT and  $MAGT1^{-/-}TUSC3^{-/-}$  samples. **(c)** Metabolic pulse chase labelling of different  
 404 NKG2D constructs, containing just one glycosylation site. Quantified values below gel lanes represent the  
 405 average number of glycans for the respective reporter ( $n = 3$ ). EH indicates endoglycosidase H treatment.

406

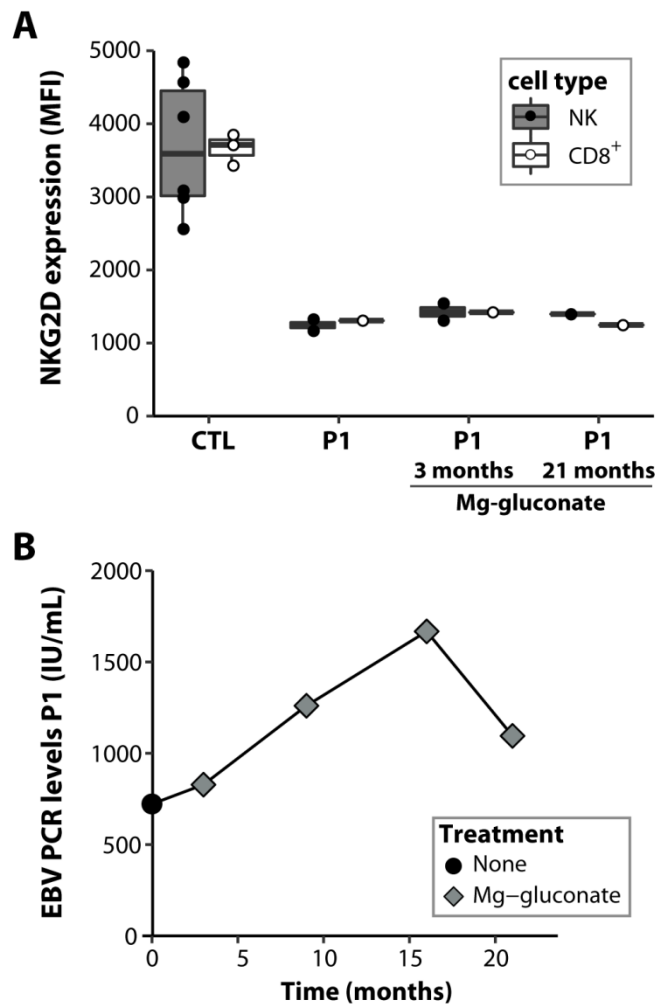


407

408 **Fig. 2 Steady state levels of NKG2D**

409 **(a)** The different HEK293 cell lines were cotransfected in regular DMEM with NKG2D-Myc-DDK and DAP10-Myc-  
 410 DDK constructs and analysed for protein steady state levels of NKG2D 48h later by immunoblotting **(b)** in  
 411 DMEM supplemented with 5 mM MgSO<sub>4</sub>. The asterisk depicts a nonspecific band co-migrating with NKG2D.  $\beta$ -  
 412 Tubulin was used as a loading control. Values represent averaged values normalised to the WT control of each  
 413 condition (n = 3). **(c)** Relative abundance of the fully glycosylated NKG2D isoform in untreated and Mg<sup>2+</sup> treated  
 414 cells, normalised to the respective WT. Error bars depict the standard deviation. (Paired Student's t test: \*=  
 415 p<0.05; \*\*= p<0.005, \*\*\*= p<0.0005; ns = not significant).

416



417

418 **Fig. 3 Effects of *in vivo* Mg<sup>2+</sup> supplementation for patient 1**

419 **(a)** Median fluorescence index (MFI) of NKG2D cell surface expression on NK (n=6) and CD8<sup>+</sup> (n=3) control (CTL)  
 420 and patient (P1) cells. For P1, levels were measured before treatment and after 3 or 21 months of 3g Mg-  
 421 gluconate per day supplementation. Gating strategy is described in **Fig. S3**.

422 **(b)** EBV (Epstein-Barr virus) PCR levels (IU/mL) of P1 measured over time (diamond squares indicate  
 423 magnesium supplementation).

424

425 **Abbreviations**

426 CDG, Congenital Disorders of Glycosylation; EH, endoglycosidase H; EBV, Epstein-Barr virus;

427 KO, knock out; MFI, median fluorescence index;  $Mg^{2+}$ , magnesium; OST,

428 oligosaccharyltransferase; WT, wild type; XMEN, X-linked immunodeficiency with  $Mg^{2+}$

429 defect, Epstein-Barr virus infection and neoplasia

430



1 **Supplementary data**

2  
3 **Title:**

4 **Lack of NKG2D in MAGT1-deficient patients is caused by hypoglycosylation**

5  
6 **Authors:** Eline Blommaert<sup>1</sup>, Natalia A. Cherepanova<sup>2</sup>, Frederik Staels<sup>3</sup>, Matthew P. Wilson<sup>1</sup>,  
7 Jaak Jaeken<sup>4</sup>, François Foulquier<sup>5</sup>, Reid Gilmore<sup>6</sup>, Rik Schrijvers<sup>3</sup> and Gert Matthijs<sup>1</sup>

8  
9 <sup>1</sup>Laboratory for Molecular Diagnosis, Center for Human Genetics, KU Leuven, 3000 Leuven, Belgium

10 <sup>2</sup> Department of Psychiatry, University of Massachusetts Medical School, 01545 Shrewsbury, MA, USA

11 <sup>3</sup> KU Leuven department of microbiology, immunology and transplantation, Allergy and Clinical  
12 Immunology research group, KU Leuven, 3000 Leuven, Belgium

13 <sup>4</sup> Department of Pediatrics, Center for Metabolic Diseases, KU Leuven, 3000 Leuven, Belgium

14 <sup>5</sup> Univ. Lille, CNRS, UMR 8576 – UGSF - Unité de Glycobiologie Structurale et Fonctionnelle, F- 59000 Lille,  
15 France

16 <sup>6</sup> Department of Biochemistry and Molecular Pharmacology, University of Massachusetts Medical School,  
17 01655 Worcester, MA, USA

18  
19  
20 **Corresponding author:** Gert Matthijs, Herestraat 49 O&N 1 Box 606, 3000 Leuven, Belgium, +32  
21 16 34 60 70, gert.matthijs@kuleuven.be

22  
23  
24 **This PDF files includes:**

25 Clinical synopsis of patient 1

26 Figure S1-3

27 Table S1

28

## 29 **Clinical synopsis of patient 1**

30 Patient 1 (also referred to as patient 3 (P3) in Blommaert et al. 2019) is a 20-year-old Caucasian  
31 male, born from non-consanguineous parents (pedigree depicted in **Fig. S2**). The patient presented  
32 with an Epstein-Barr virus (EBV) primary infection at the age of 2, necessitating admission to the  
33 paediatric intensive care unit due to deterioration of his general condition, a petechial rash and  
34 pancytopenia with hypertriglyceridemia and mild coagulation abnormalities. Next, also a  
35 maculopapular rash and generalized oedema was noted. Bone marrow aspirate demonstrated  
36 absence of malignancy and mostly abundant granulocyte formation. Oxygen, antibiotics and IV fluid  
37 treatment was installed with a favourable evolution except for persistent hepatomegaly. A liver  
38 biopsy, performed after his stay at the paediatric intensive care unit, did not show hepatitis or  
39 hematophagocytosis. Serum ferritin, soluble CD25 was not determined. This episode was  
40 interpreted as a primary EBV infection, complicated with a macrophage activation syndrome.  
41 Afterwards, a persistent EBV viremia was observed (**Table S1** and **Fig. 3B**). Since the age of 8,  
42 recurrent herpes simplex virus (HSV) stomatitis episodes, treated with acyclovir, and HSV labialis  
43 (every 2-3 months) were noted. During childhood (age 10 years and onwards) he had recurrent  
44 warts (predominant on the hands and arms) that subsided later in adolescence. Recurrent furuncles  
45 were noted in childhood and adolescence, and post-appendectomy infection required IV antibiotics  
46 (age 10 years). Finally, he mentioned upper respiratory tract infections, sporadically leading to  
47 antibiotic treatment via his general practitioner (GP).

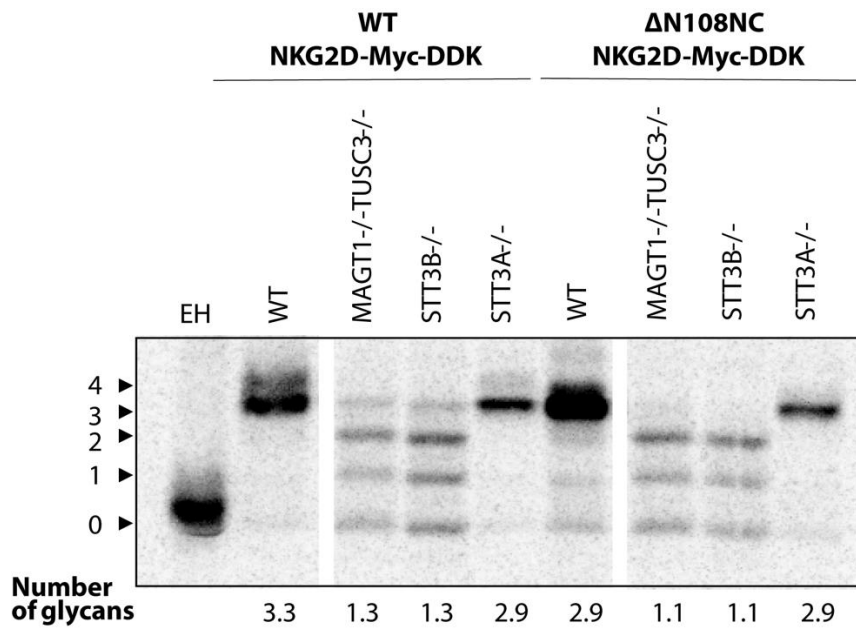
48 Clinical examination was normal at time point T0 (17 years, 10 months). Of note, no palpable glands  
49 were noted although recurrent enlarged cervical lymph nodes were mentioned and ultrasound  
50 revealed a spleen diameter at the upper limit of normal (cranial-caudal diameter of 12.4 cm, age 19,  
51 body height 1.77 m). Laboratory results demonstrated mild neutropenia, thrombocytopenia, lowered  
52 IgG (7.46 g/L, normal range (NR) 7.51-15.60), elevated transaminases, and persistent EBV-viremia  
53 (**Table S1** and **Fig. 3B**). Further immunological evaluation demonstrated normal total lymphocyte, T-,  
54 and NK-cell count, elevated CD19<sup>+</sup> B-cell count (1542/ $\mu$ L, NR 82 - 0.476), consisting predominantly of  
55 naive (94% CD27<sup>-</sup>IgM<sup>+</sup>) B-cells, next to lowered IgM-memory (CD27<sup>+</sup>IgM<sup>-</sup>, 2.2%) and switched  
56 memory (CD27<sup>+</sup>IgM<sup>-</sup>, 2.8%) B-cells. CD4, CD8 T-cell, regulatory T-cell (8.4% CD4<sup>+</sup>CD25<sup>+</sup>CD127<sub>low</sub>)  
57 counts were normal. CD4:CD8 ratio was normal (0.89, NR 0.80-3.50). Double negative T-cells (DNT,  
58 alpha-beta T-cell receptor CD3<sup>+</sup>CD4<sup>-</sup>CD8<sup>-</sup>) were elevated (2.8% of CD3), naive T-cell (CD27<sup>+</sup>CD45RA<sup>+</sup>)  
59 count was 62% of CD3 positive cells. Lymphocyte proliferation rate was normal using HSV, varicella  
60 zoster virus, or PHA (index for HSV was 14.03, for varicella zoster virus 159.41, for PHA 61.12;  
61 normal > 5.0). Stimulation with anti-CD3/CD28 on frozen or fresh PBMCs did not result in  
62 proliferation of patient lymphocytes.

63 The patient received standard vaccinations including vaccination with live attenuated measles,  
64 mumps, and rubella uneventfully and resulting in normal or near-normal serologic responses (anti-  
65 measles IgG 650 mIU/mL; anti-rubella IgG 8.4 IU/mL, normal >10.0 mIU/mL; anti-hepatitis B surface  
66 antigen IgG 11.5 mIU/mL, normal  $\geq$  10.0 mIU/mL; measured at the age of 19 years). Pneumococcal  
67 polysaccharide vaccination was refused. Varicella zoster virus and CMV serology demonstrated past  
68 infection, PCR for persistent CMV viremia was negative. PCR for polyoma virus (BK/JC virus) in urine  
69 was positive (> 8 log copies/mL).

70 Next generation sequencing revealed a pathogenic variant in the X-linked *MAGT1* gene (c.938T>G,  
71 p.Leu313\*) at 17 years of age (Blommaert et al. 2019). Given the clinical features of persistent EBV  
72 viremia, macrophage activation syndrome during primary infection, decreased NKG2D expression  
73 (Blommaert et al. 2019) and the rare, previously unreported nor identified (ExAC database,  
74 gnomAD, 1000 genomes) variant in *MAGT1*, a diagnosis of X-linked immunodeficiency with  
75 magnesium defect, EBV infection, and neoplasia (XMEN) disease was made.

76 He was treated with oral magnesium supplementation from the age of 17 years and 10 months  
77 onwards using 3 g of Mg<sup>2+</sup> gluconate (containing 162 mg Mg<sup>2+</sup>, Ultra-Mg®, Melisana) per day.  
78 Increasing the frequency to twice or three times per day led to gastro-intestinal intolerance.  
79 Magnesium threonate, as was previously reported as a therapy for XMEN patients (Chaigne-  
80 Delalande et al. 2013), was not initiated because of unavailability via the local hospital pharmacy.  
81 Since magnesium supplementation, he noted a drop in upper respiratory tract infections and HSV  
82 stomatitis episodes (although from hindsight this was already absent the year before). EBV viremia  
83 was deemed to be non-responsive to magnesium supplementation (**Fig. 3B**). Of note, elevated  
84 transaminases were observed throughout the follow-up with a temporary flare-up coinciding with  
85 the start of magnesium supplementation. No changes in total serum magnesium were noted  
86 throughout the follow-up (**Table S1**). Subjectively, he felt his general condition was comparable to  
87 that of his peers. Although he was reluctant for a frequent clinical follow-up, adherence to  
88 magnesium supplementation was high, possibly suggesting (at least subjective) efficacy.

89



91

92

93 **Figure S1: The N<sub>108</sub>NC glycosylation site is suboptimal.**94 Metabolic pulse chase labelling of the WT NKG2D-Myc-DDK and the ΔN<sub>108</sub>NC NKG2D-Myc-DDK construct, in

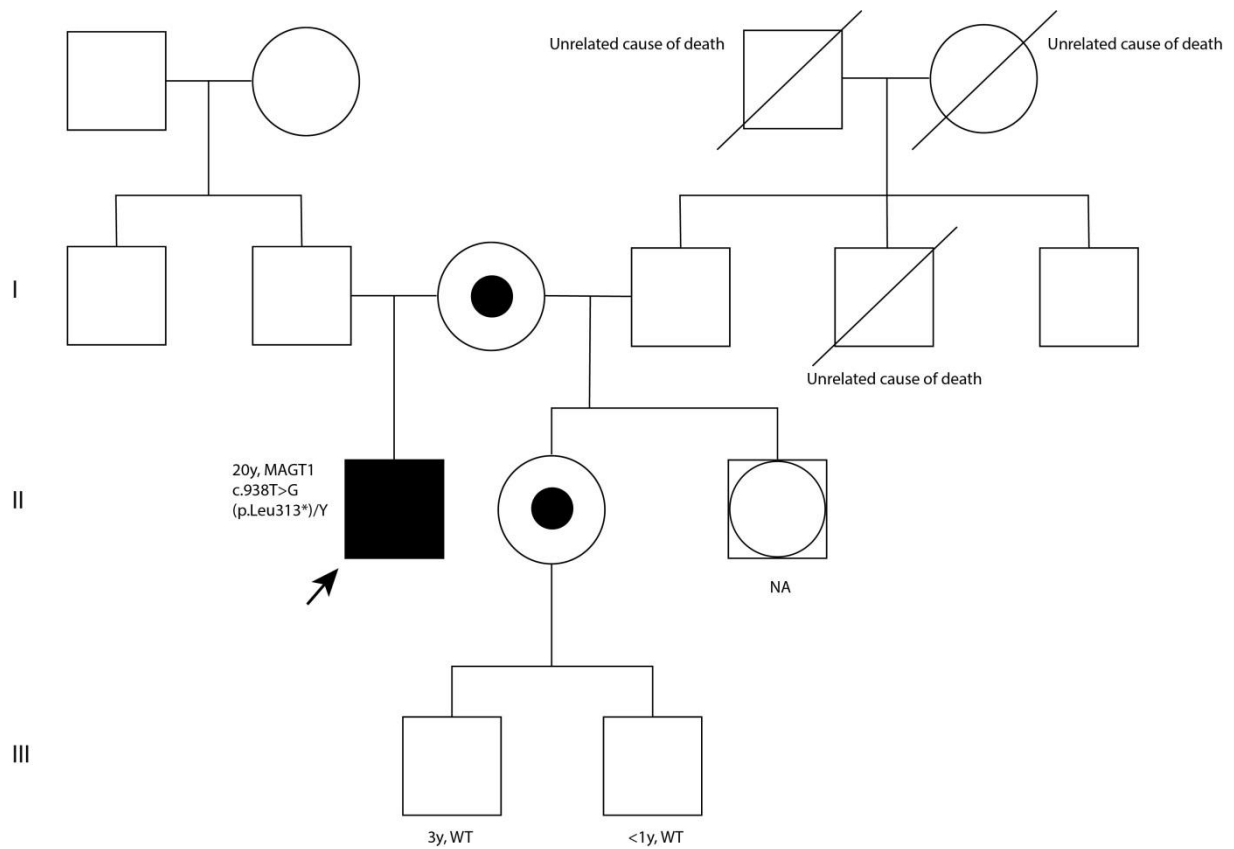
95 different HEK293 engineered cell lines. Quantified values are shown below gel lanes and represent the number

96 of glycans for the respective reporter. EH indicates Endoglycosidase H treatment, and serves as a mobility

97 marker. White lanes between samples indicates where the figure was spliced.

98

99

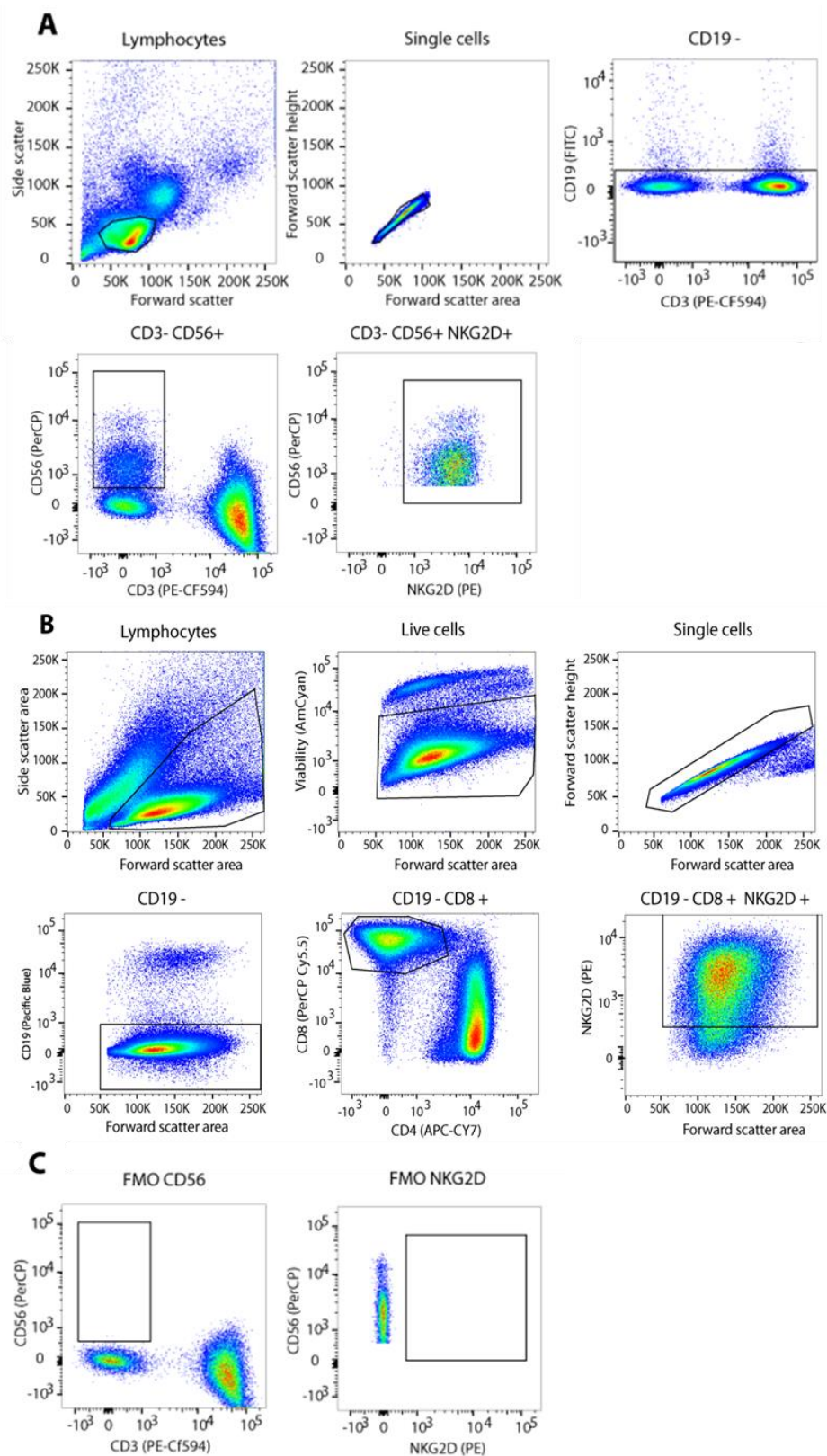


100

101 **Figure S2: Pedigree of patient 1.**

102 Index case (II.1) is from Caucasian, European descent. No consanguinity was noted and no other affected male  
 103 family members were identified. Medical history of the other family members was negative except for  
 104 recurrent nasal and labial herpes simplex virus infection in his half-sibling (II.2, carrier of *MAGT1* c.938T>G),  
 105 which was regarded as non-exceptional.

106 *Abbreviations:* WT, wild type; NA, not available.



107

108 **Figure S3: Gating strategy for NKG2D expression levels on NK cell surface.**

109 (A) First, PBMC were selected on both size and singularity. Next, CD19 and CD3 negative cells were gated on  
 110 expression of CD56 to identify NK cells. Finally, NK cells were gated for expression of NKG2D.

111 (B) First, PBMC were selected on size, living cells and singularity. Next, CD19 negative cells were gated on  
 112 expression of CD8 to identify CD8+ cells. These cells were gated for expression of NKG2D;

113 (C) Fluorescence Minus One (FMO) for CD56 and NKG2D to determine gates for both proteins.

114 **Table S1: Summary of clinical values for P1 at different time points.**

115 Values outside the normal range are marked in red. EBV = Epstein-Barr Virus, Treg = T regulatory cells

	Reference value	+644 days	+483 days	+287 days	+93 days	+63 days	T0 (17y 10months)
<b>White blood cells</b>	4-10 x10 <sup>9</sup> /L	4.46	6.43	5.17	4.58	4.59	4.92
<b>Platelets</b>	150-450x10 <sup>9</sup> /L	132	196	142	177	179	179
<b>Hemoglobin</b>	13.0 -16.0 g/dl	14.0	14.4	14.0	13.8	15.0	14.6
<b>C-reactive protein</b>	≤5 mg/L	0.9	1.0	0.5	1.9	0.8	0.3
<b>Neutrophils</b>	2.5-7.8 x10 <sup>9</sup> /L	1.5	2.6	1.8	1.4	1.2	1.6
<b>Lymphocytes</b>	20-50 %	58.7	51.6	55.7	59.2	68	59.6
<b>CD19<sup>+</sup></b>	0.082-0.476 x10 <sup>9</sup> /L	1.261	1.619	1.443			1.542
<b>CD4<sup>+</sup></b>	0.455-1.885 x10 <sup>9</sup> /L	0.572	0.646	0.554			0.531
<b>CD8<sup>+</sup></b>	0.219-1.124 x10 <sup>9</sup> /L	0.578	0.741	0.632			0.599
<b>CD4/CD8 ratio</b>	0.8-3.5	0.99	0.87	0.88			0.89
<b>NK (CD3<sup>+</sup>;CD56<sup>+</sup>)</b>	4-30 %	4.3	5.7	4.7			4.6
<b>Treg (CD4<sup>+</sup>;CD125<sup>+</sup>CD127<sub>low</sub>)</b>	5-12 % of CD4+						8.4
<b>IgG</b>	7.51-15.6 g/l	8.72	8.39	7.46			8.44
<b>IgA</b>	0.82-4.53 g/L	0.46	0.60	0.48			0.52
<b>IgM</b>	0.46-3.04 g/L	0.52	0.48	0.41			0.41
<b>Serum magnesium</b>	0.63-1.05 mmol/L	0.78	0.82	0.78		0.82	
<b>EBV viremia</b>	EBV PCR IU/ml	1095	1667	1260		828	772
<b>Aspartate transaminase</b>	≤38 U/L	38		33	57	81	24
<b>Alanine transaminase</b>	≤41 U/L	76		57	95	100	42
<b>Gamma glutamyl transferase</b>	≤60 U/L	20		19	20	21	19
<b>Alkaline phosphatase</b>	40-130 U/L	112		121	133	149	145
<b>Body mass index</b>	18.5-25 kg/m <sup>2</sup>	22.4	22.9	23.2	22.9		22.1